Atmospheric River Event over the Eastern Pacific in February 2014: Analysis and Climatological Context

Deveshi Buch

Vista del Lago High School, Folsom, CA

INTRODUCTION

Atmospheric Rivers

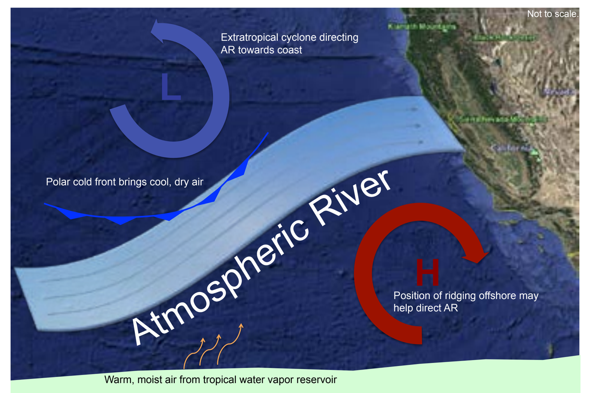

Long, filamentary corridors called Atmospheric Rivers (ARs) are responsible for >90% of poleward transport of water vapor across the mid-latitudes [Zhu and Newell 1998; Neiman et al. 2008 (Met.)]. Typically, an AR is associated with the warm conveyor belt (WCB) of an extratropical cyclone. An AR has the following properties [Ralph et al. 2004, 2005; Neiman et al., 2008 (Dia.)]: (1) a narrow band of high specific humidity, (2) high wind speeds in a pre-cold-frontal low level jet (around 1 km MSL) occupying a portion of the WCB, and (3) low-level instability. ARs are contiguous regions ≥2000 km in length, ≤1000 km in width, Integrated Water Vapor (IWV) ≥20 kgm^{-2} (mm), and Integrated Vapor Transport (IVT) ≥250 $kgm^{-1}s^{-1}$ [Ralph et al. 2004; Dettinger et al. 2011; Rutz et al. 2014]. Over the United States, IVT appears to be more useful than IWV in characterizing ARs because of the inclusion of zonal and meridional wind speeds [Rutz et al. 2014; Nayak et al. 2014].

Impacts of Atmospheric Rivers: Costs & Benefits

Left: http://content.time.com/time/specials/packages/article/0,28804,2070796_2070798_2070791,00.html
Center: http://www.sfgate.com/bayarea/article/Storm-rages-on-bringing-widespread-flooding-and-6884460.php
Right: http://www.shastalake.com/shastadam/

AR events are responsible for bringing significant precipitation to Western North America and replenishing water resources, but are also notorious for catastrophic floods. ARs have also been linked to extreme precipitation and flooding over W. Europe, E. United States, and other parts of the world [Rutz et al. 2015]. California's water supply depends greatly upon ARs, which provide 25-50% of a water-year's precipitation, often in a few short events [Dettinger et al. 2011]. 90% of California's heaviest 1-3 day precipitation events are linked to ARs [Ralph et al. 2010]. 40% of droughts in N. California ended with an AR [Dettinger 2013].

ARs: An Active Area of Research

Right: [Zhu and Newell 1998]
Below: http://tropic.ssec.wisc.edu/real-time/mimic-tpw/global/main.html

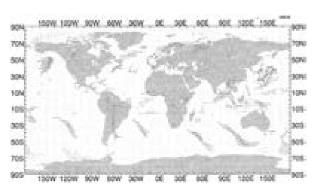

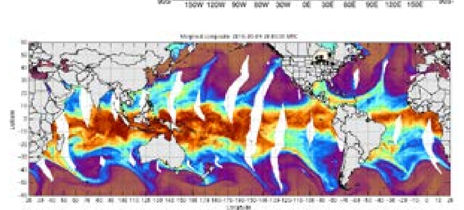

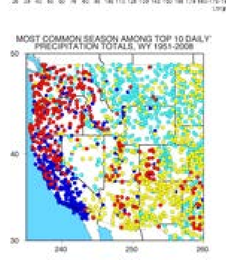

Most common season among top 10 daily precipitation totals for the western U.S. [Ralph et al. 2014]. It can be observed from this plot that precipitation is most common in the California region in the cold season, from October to March.

Right: http://www.livescience.com/49700-flying-into-atmospheric-rivers-study.html

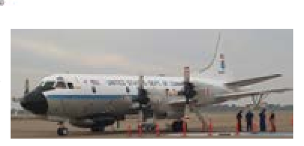

The structure of ARs has been studied and modeled [Ralph et al. 2004, 2005]. Studies on the climatology of ARs [Lavers et al. 2012, Neiman et al. 2008, Ralph et al. 2013] explore the average freqency and duration of AR events. One study found that ARs impact the West Coast of the U.S. in the pre- (post-) cold frontal environment in winter (summer), IWV (IVT) is stronger for summer (winter) ARs, and winter ARs produce about twice as much precipitation as all storms [Neiman et al. 2008]. The skill of climate models at predicting ARs has been extensively studied [Wick et al. 2013; Nayak et al. 2014]. In general, models can predict the occurrence of ARs up to 10 days in advance; however, timing and location of landfall, as well as intensity of precipitation, are more challenging to predict. The link with synoptic scale dynamics is still poorly understood, although studies have investigated the relationship of ARs and the Madden-Julian Oscillation (MJO), North Atlantic Oscillation (NAO), El Nino-Southern Oscillation (ENSO), and the Pacific-Decadal Oscillation (PDO) [Bao et al. 2006; Lavers et al. 2012, 2013; Ralph et al. 2011]. Studies have also analyzed how deeply inland ARs are able to carry their vapor flux [Rutz et al. 2015]. An AR observation (ARO) network designed to collect and analyze AR data has been implemented in California as a joint project between CA DWR, NOAA, and Scripps Inst. of Oceanography at UCSD. Bodega Bay (BBY) is one such ARO site.

OBJECTIVES OF THIS STUDY

(1) Perform a case study of a significant AR event occurring in February 2014 over the Eastern Pacific and the West Coast of the United States. Analyze the evolution, characteristics, and impact of the Feb. 2014 AR.

(2) Consider the event in a climatological context. Evaluate AR events occurring in the month of February over the 20-year period from 1996-2015.

MATERIALS & METHODS

The case study of the Feb. 2014 AR event is based on data from NASA Modern-Era Retrospective Analysis for Research and Applications (MERRA) at a resolution of 2/3 × 1/2 deg. Data for the climatological study is obtained from European Centre for Medium-Range Weather Forecasts (ECMWF) ERA-Interim reanalysis datasets for the month of February over the 20-year period from 1996-2015 at a resolution of 3/4 × 3/4 deg. Dates of observed landfalling ARs for WY 1998-2008 impacting CA (32.5°N-41.0°N) are from SSM/I ascending and descending passes [Dettinger et al. 2011]. AR dates for 1996-1997 and 2009-2015 are calculated here based on ECMWF reanalysis with the constraint of IWV ≥20 mm for observations 12 hrs apart. Files are manipulated using NetCDF Data Operators (NCO). Data processing, analysis, and plot generation are performed by custom Python code using Numerical Python (NumPy) and the NetCDF4, Matplotlib, and Basemap modules. Panoply was used for data visualization and case study duration charts. For an overview of the processing flows, see Fig. 8.

IWV (Integrated Water Vapor) is mathematically defined as:

$$\mathrm{IWV} = \frac{1}{g}\int q\,\mathrm{d}p$$

where g is the gravitational acceleration in ms^{-2}, q is the specific humidity in $kgkg^{-1}$, and $\mathrm{d}p$ in Pa is the pressure delta between adjacent pressure levels [Rutz et al. 2014].

IVT is vertically integrated horizontal water vapor transport [Zhu and Newell 1998; Neiman et al. 2008 (Dia.); Lavers et al. 2012; Nayak et al. 2014] and is mathematically defined as:

$$\mathrm{IVT} = \sqrt{\left(\frac{1}{g}\int qu\,\mathrm{d}p\right)^2 + \left(\frac{1}{g}\int qv\,\mathrm{d}p\right)^2}$$

where the additional terms u and v are the zonal and meridional winds in ms^{-1}.

RESULTS & DISCUSSION

(PART I) CASE STUDY OF SPECIFIC AR

AR Characteristics

AR1: California: 08 Feb 2014

AR threshold criteria:
Width: ≤1000 km
Length: ≥2000 km
IWV: ≥20 mm
IVT: ≥250 $kgm^{-1}s^{-1}$

Fig. 1

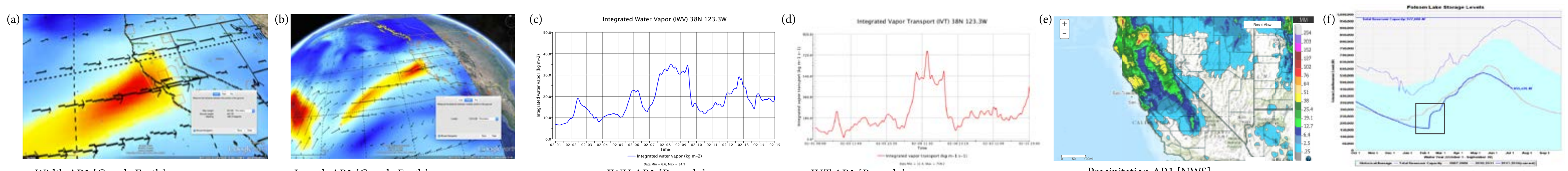

(a) Width AR1 [Google Earth] ~450 km
(b) Length AR1 [Google Earth] ~2600 km
(c) IWV AR1 [Panoply] Max: ~35 mm
(d) IVT AR1 [Panoply] Max: ~759 $kgm^{-1}s^{-1}$; Duration ~55 hrs
(e) Precipitation AR1 [NWS]
(f) CA RESERVOIR LEVELS [CA DWR] ~100,000 AF increase

AR2: Oregon-Washington: 12 Feb 2014

Fig. 2

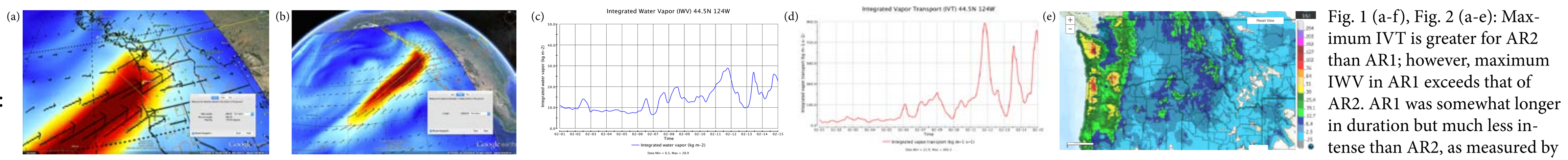

(a) Width AR2 [Google Earth] ~700km
(b) Length AR2 [Google Earth] ~3000 km
(c) IWV AR2 [Panoply] Max: ~29 mm
(d) IVT AR2 [Panoply] Max: ~886 $kgm^{-1}s^{-1}$; Duration ~38 hrs
(e) Precipitation AR2 [NWS]

Fig. 1 (a-f), Fig. 2 (a-e): Maximum IVT is greater for AR2 than AR1; however, maximum IWV in AR1 exceeds that of AR2. AR1 was somewhat longer in duration but much less intense than AR2, as measured by IVT. Significant precipitation resulted from AR1 and AR2. This AR event increased Folsom Lake storage levels by ~100,000 AF.

California Event: 08-10 Feb 2014

The 500 and 850 hPa geopotential height and IVT/IWV charts, Fig. 3 (a-d), show the upper-level cyclone and anticyclone over the central and eastern Pacific on 08 Feb 2014. There is a closed cyclone at ~50°N,160°W and an anticyclone at ~25°N,125°W. In (a) and (b), the wind direction corresponds to the flow of moisture out of the tropical-equatorial reservoir. Fig. 3 (c) and (d) show the entrainment of the moisture in a channel directed at California. The AR is visible making landfall in (c) and (d) at ~38°N,123°W, with core IVT values exceeding 900 $kgm^{-1}s^{-1}$ and IWV values exceeding 40 mm. Fig. 4 shows (a) GOES WEST Visible, (b) GOES WEST Infrared, and (c) SSM/I for the 08 Feb. 2014 AR.

Fig. 3

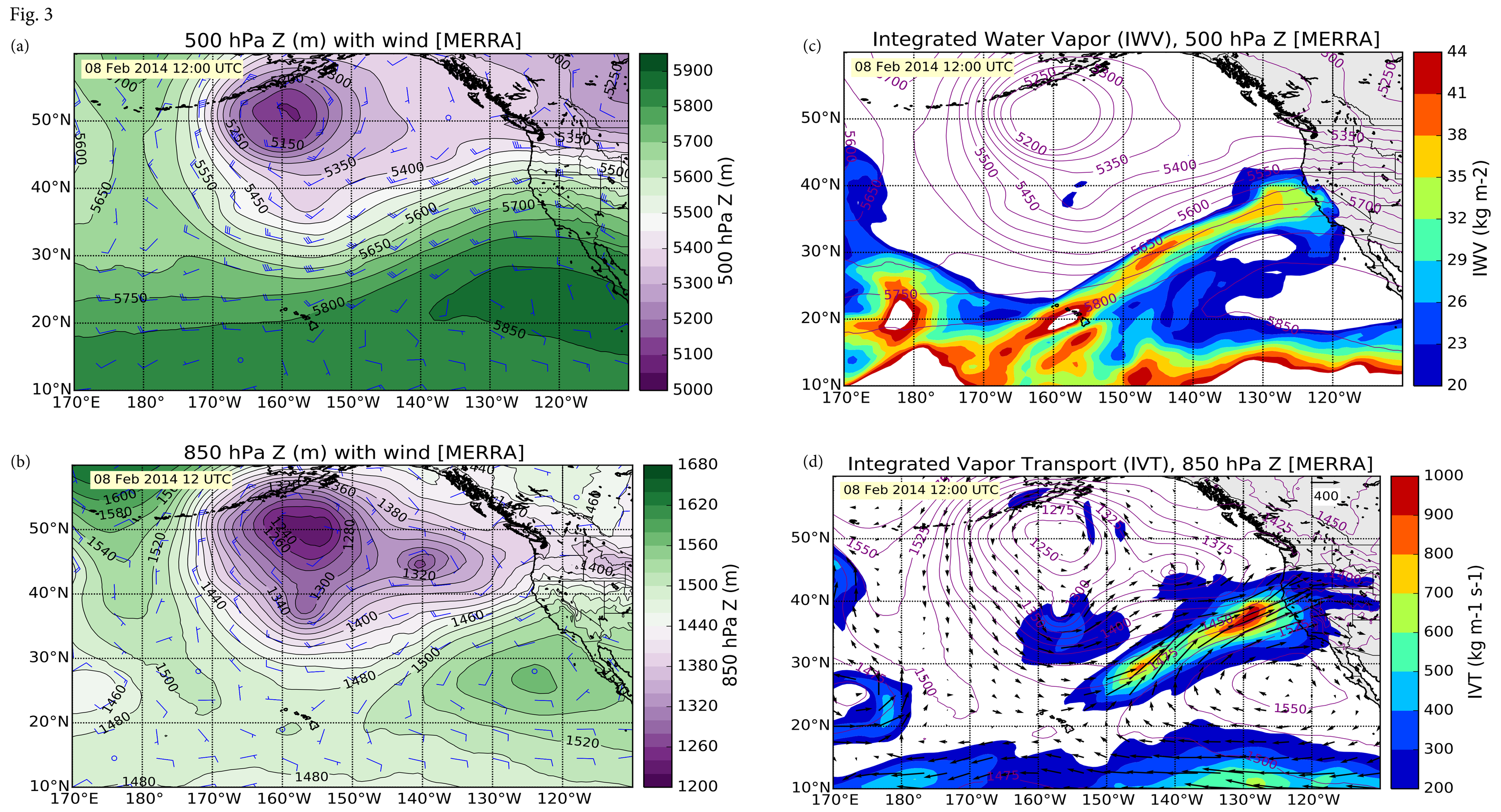

Fig. 4

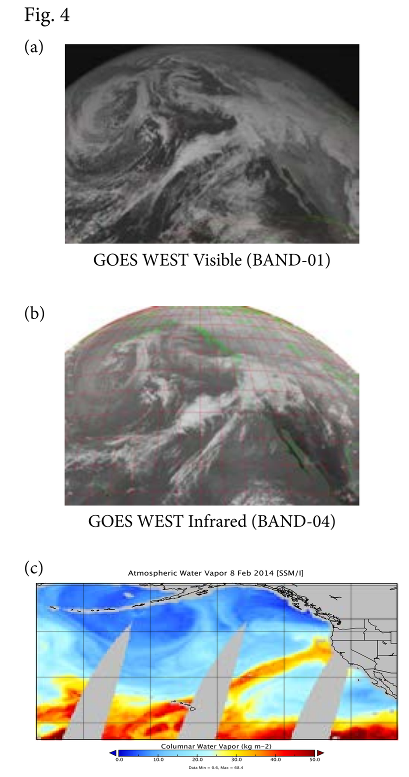

(a) GOES WEST Visible (BAND-01)
(b) GOES WEST Infrared (BAND-04)
(c) SSM/I

(PART II) AR CLIMATOLOGY

Fig. 5

#	WY1996	WY1997	WY1998	WY1999	WY2000	WY2001	WY2002	WY2003	WY2004	WY2005	WY2006	WY2007	WY2008	WY2009	WY2010	WY2011	WY2012	WY2013	WY2014	WY2015
1	19960203		**19980202**	19990207				20030212	**20040216**		20060227	20070209		20090222	20100224		20120207		**20140208**	**20150206**
2	**19960204**		**19980203**						20040217			20070210		20090223					**20140209**	**20150207**
3	19960205		**19980205**																20140210	**20150208**
4	19960216																			
5	19960217																			
6	19960219																			

Fig. 6

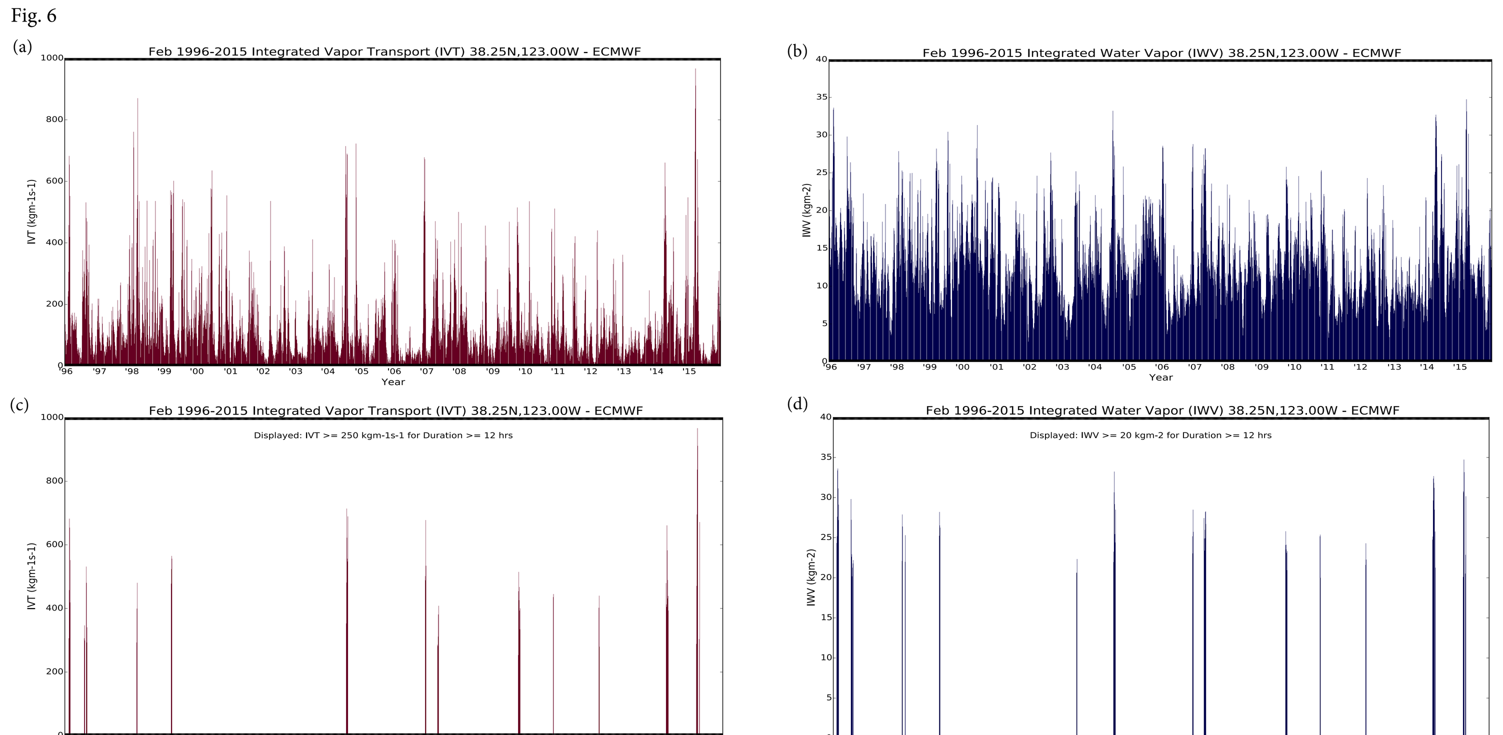

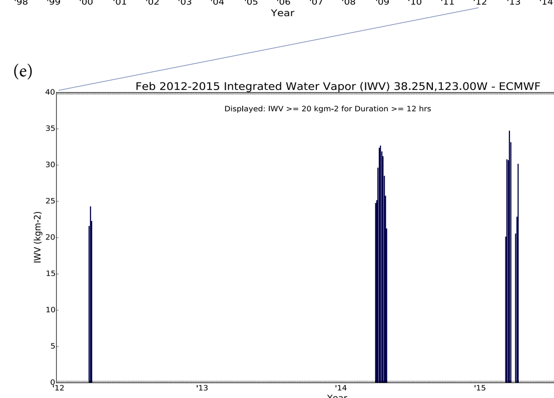

From Fig. 5, it can be observed that the Feb. 2014 AR event is one of five significant AR events (in bold), with IWV ≥30 mm. The 20-year data for IWV and IVT in Fig. 6 (a) and (b) are for Feb. 1996-2015, at 6 hr intervals, for 38.3°N,123.0°W. An expanded view of the 2012-2015 data is in Fig. 6 (e). An algorithm was developed in Python to filter this raw data to meet a threshold of ≥20 kgm^{-2} (IWV) and ≥250 $kgm^{-1}s^{-1}$ (IVT), to expose those values that likely represent AR events. The AR events in Fig. 5 appear to be present in the filtered data. Note that values of IWV/IVT that meet criteria do not solely establish the presence of an AR. Data in Fig. 6 (a-d) are for a location in proximity to the Bodega Bay Atmospheric River Observatory in California, whereas the AR events recorded in Fig. 5 correspond to 32.5°N-41.0°N.

Fig. 7

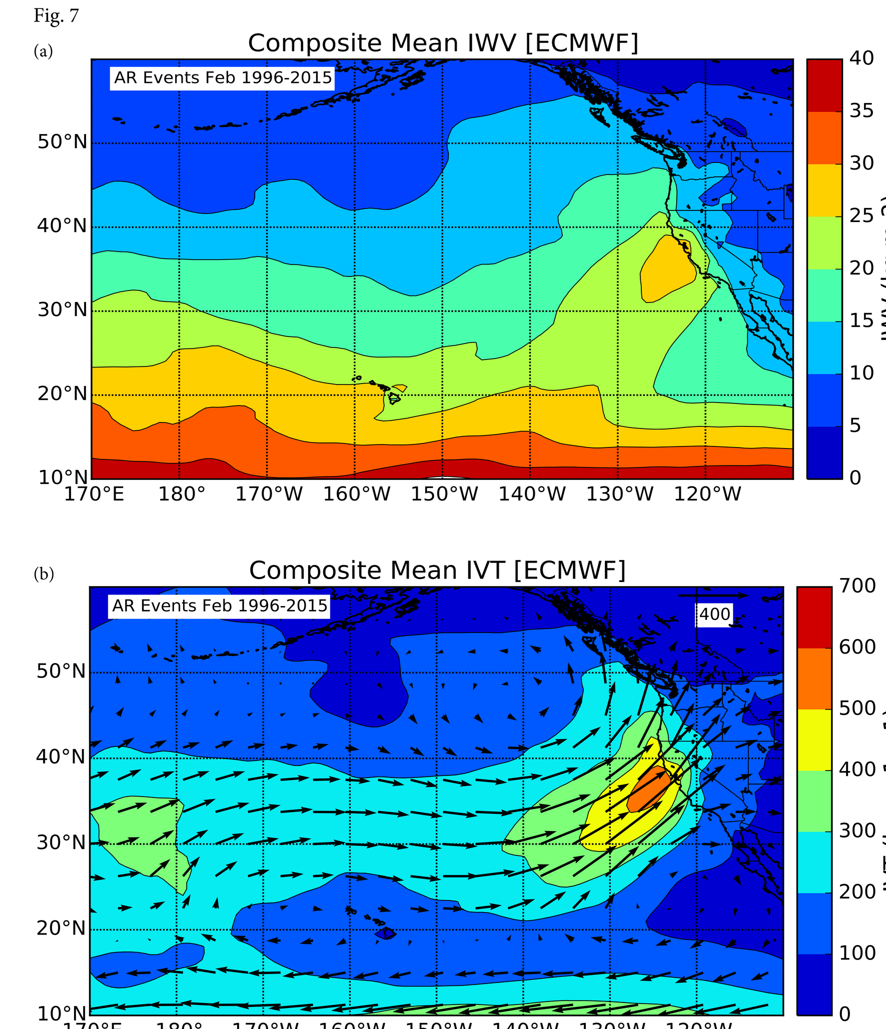

Fig. 7 (a) and (b) show the composite mean IWV and IVT values for February ARs in the 1996-2015 period. Peak IWV of 25-30 mm and peak IVT of 500-600 $kgm^{-1}s^{-1}$ are observed at the core of the composite AR.

Fig. 8

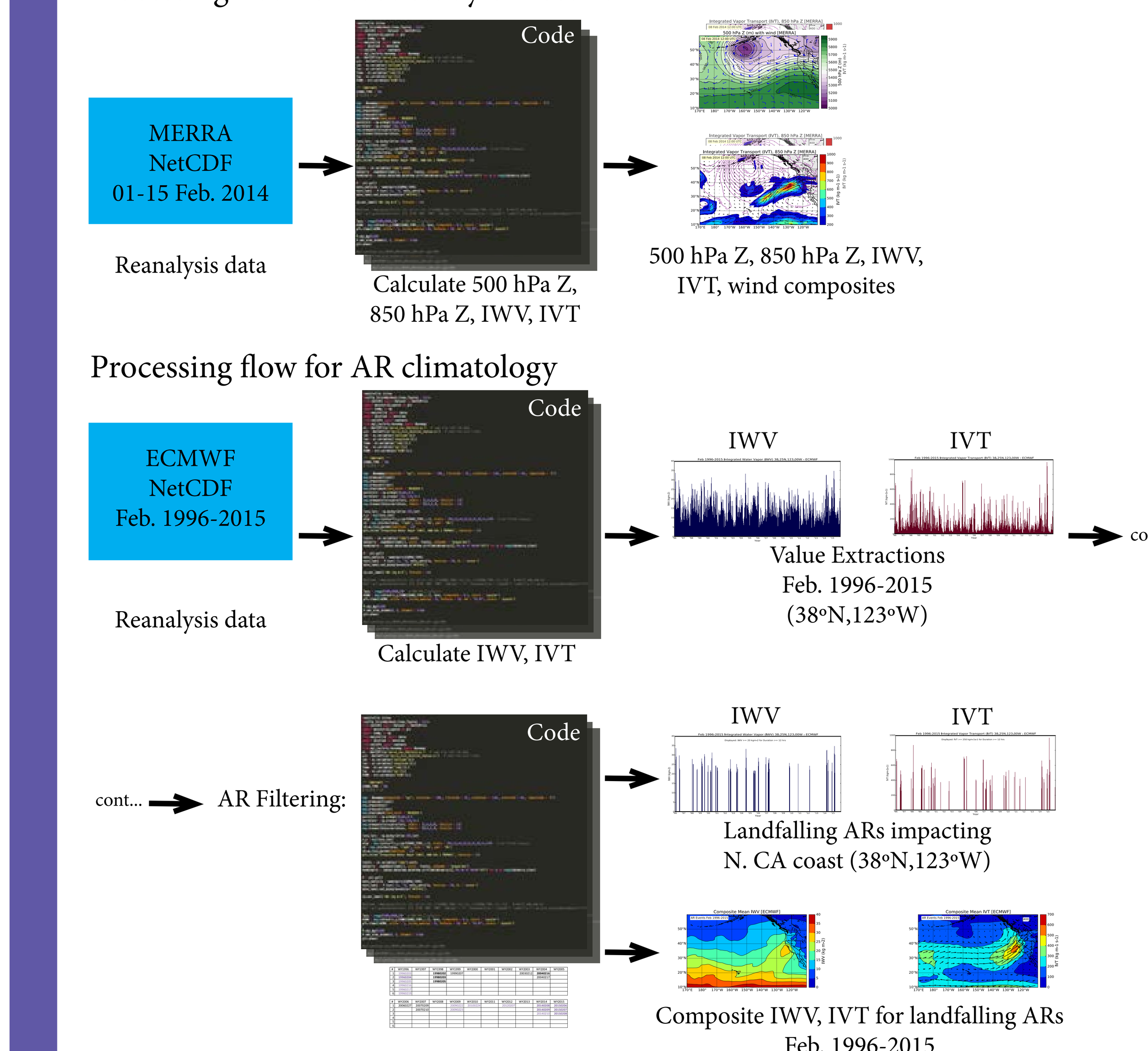

Feb. 2013 Observations

Fig. 9

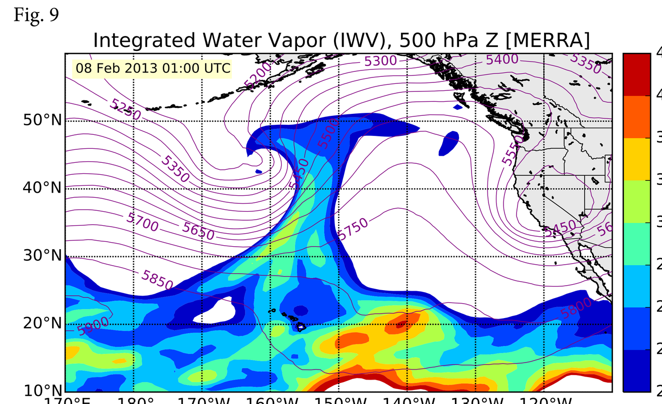

It can be observed from Fig. 5 that there was a dearth of ARs during Feb. 2013. This may have been due to the presence of a ridge visible at ~30-40°N & ~140°W (see Fig. 9), also noted in [Swain et al. 2014], possibly diverting ARs northward. A similar region of high pressure near California may have diverted ARs in the following (not shown): 7 Feb. 2000, 11 Feb. 2001, 22 Feb. 2002, 24 Feb. 2005, 14 Feb. 2008, and 05 Feb. 2011.

CONCLUSIONS

The evolution, transport, and landfall of a major AR event over the Eastern Pacific in February 2014 were analyzed. The AR is characterized by high levels of IWV (~35 mm) and IVT (~759 $kgm^{-1}s^{-1}$) and resulted in significant precipitation. Analysis of the synoptic-scale conditions shows upper-level extratropical cyclones and anticyclones guiding the flow of vapor transport in a narrow channel ~450 km in width and ~2600 km in length. This AR event is considered in a climatological context using IWV and IVT data for the month of February from 1996-2015. It is observed that the February 2014 AR event is one of five significant events in the 20-year period, as measured by IWV ≥30 mm. A composite mean of the IVT values is also calculated, showing peak IVT of 500-600 $kgm^{-1}s^{-1}$ at the core of the composite AR. An observed dearth of ARs in Feb. 2013 appears to be linked to the presence of a ridge, possibly diverting the flow away from California. Regional characterizations such as this study can assist in gaining a better understanding of the formation of ARs, their probable trajectories, and impact at landfall. Our ability to forecast these extreme phenomena is crucial for water resource management, flood planning, agriculture, and the economy. Future work for this study includes further development of the algorithms to identify and characterize ARs in climate datasets.

REFERENCES

Bao, J. W., S. A. Michelson, P. J. Neiman, F. M. Ralph, and J. M. Wilczak, 2006: Interpretation of enhanced integrated water vapor bands associated with extratropical cyclones: Their formation and connection to tropical moisture. *Mon. Wea. Rev.*, 134(4), 1063-1080.

Dettinger, M. D., F. M. Ralph, T. Das, P. J. Neiman, and D. R. Cayan, 2011: Atmospheric rivers, floods and the water resources of California. *Water 3*, no. 2: 445-478.

——, 2013: Atmospheric rivers as drought busters on the US West Coast. *J. Hydrometeor.*, 14(6), 1721-1732.

Lavers, D. A., G. Villarini, R. P. Allan, E. F. Wood, and A. J. Wade, 2012: The detection of atmospheric rivers in atmospheric reanalyses and their links to British winter floods and the large-scale climatic circulation. *J. Geophys. Res.*, 117, D20106.

——, ——, 2013. The nexus between atmospheric rivers and extreme precipitation across Europe. Geophys. Res. Lett. 40, 3259–3264. doi: 10.1002/grl.50636

Nayak, M. A., G. Villarini, and D. A. Lavers, 2014: On the skill of numerical weather prediction models to forecast atmospheric rivers over the central United States." *Geophys. Res. Lett.*, 41(12), 4354-4362.

Neiman, Paul J., F. M. Ralph, G. A. Wick, Y. Kuo, T. Wee, Z. Ma, G. H. Taylor, and M. D. Dettinger, 2008: Diagnosis of an intense atmospheric river impacting the pacific northwest: Storm summary and offshore vertical structure observed with COSMIC satellite retrievals. *Mon. Weather Rev.*, 136(11), 4398–4420.

——, ——, ——, J. D. Lundquist, and M. D. Dettinger, 2008: Meteorological Characteristics and Overland Precipitation Impacts of Atmospheric Rivers Affecting the West Coast of North America Based on Eight Years of SSM/I Satellite Observations. *J. Hydrometeor.*, 9, 22–47.

Ralph, F. M., P. J. Neiman, and G. A. Wick, 2004: Satellite and CALJET aircraft observations of atmospheric rivers over the eastern North Pacific Ocean during the winter of 1997/98. *Mon.Wea. Rev.*, 132(7), 1721-1745.

——, ——, and R. Rotunno, 2005: Dropsonde observations in low-level jets over the northeastern Pacific Ocean from CALJET-1998 and PACJET-2001: Mean vertical-profile and atmospheric-river characteristics. *Mon. Wea. Rev.*, 133(4), 889-910.

——, ——, G. A. Wick, S. I. Gutman, M. D. Dettinger, D. R. Cayan, and A. B. White, 2006: Flooding on California's Russian River: Role of atmospheric rivers. *Geophys. Res. Lett.*, 33(13).

——, ——, G. N. Kiladis, K. M. Weickmann, and D. W. Reynolds, 2010: A multi-scale observational case study of a Pacific atmospheric river exhibiting tropical-extratropical connections and a mesoscale frontal wave. *Mon. Wea. Rev.*

——, ——, ——, ——, and ——, 2011: A multi-scale observational case study of a Pacific atmospheric river exhibiting tropical-extratropical connections and a mesoscale frontal wave. *Mon. Wea. Rev.*, 139, 1169–1189.

——, T. Coleman, P. J. Neiman, R. J. Zamora, and M. D. Dettinger, 2013: Observed impacts of duration and seasonality of atmospheric-river landfalls on soil moisture and runoff in coastal northern California. *J. Hydrometeor.*, 14(2), 443-459.

Rutz, J. J., W. J. Steenburgh, and F. M. Ralph, 2014: Climatological characteristics of atmospheric rivers and their inland penetration over the western United States. *Mon. Wea. Rev.*, 142(2), 905921.

——, ——, and ——, 2015: The inland penetration of atmospheric rivers over western north america: A lagrangian analysis. *Mon. Wea. Rev.*, 143(5), 1924-1944.

Swain, D., M. Tsiang, M. Haugen, D. Singh, A. Charland, B. Rajaratnam, and N. S. Diffenbaugh, 2014: The extraordinary California drought of 2013/2014: Character, context, and the role of climate change [in "Explaining Extreme Events of 2013 from a Climate Perspective"]. *Bull. Amer. Meteor. Soc.*, 95(9), 3-7.

Wick, G. A., P. J. Neiman, and F. M. Ralph, 2013: Description and validation of an automated objective technique for identification and characterization of the integrated water vapor signature of atmospheric rivers. *IEEE Trans. Geo. Rem. Sens.*, 51(4), 2166-2176.

Zhu, Y. and R. E. Newell, 1998: A proposed algorithm for moisture fluxes from atmospheric rivers. *Mon. Wea. Rev.*, 126(3), 725–735.

(Selected references shown.)

ACKNOWLEDGEMENTS

The author of this study gratefully acknowledges the guidance and support provided by Dr. Paul Ullrich, Assistant Professor of Regional Climate Modeling, Dept. of Land, Air and Water Resources, UC Davis. Many thanks to Dr. Robert B. Schmunk (NASA Goddard) for providing a special beta version of Panoply.